

Monte Carlo code-code comparison of secondary yields in processes relevant for the Mu2e experiment

S. Di Falco¹, A. Ferrari², V. Giusti³, S. Müller², V. Pronskikh⁴ and R. Rachamin²

¹INFN Pisa, Pisa, Italy ²Helmholtz-Zentrum Dresden-Rossendorf, Dresden, Germany
³University of Pisa, Pisa, Italy ⁴Fermi National Accelerator Laboratory, Batavia, IL, USA

Motivation: particle production and background control in the Mu2e experiment

The Mu2e experiment will search for the Charged-Lepton Flavor Violation (CLFV) neutrino-less Muon-to-Electron conversion in the field of a nucleus ($\mu^- + \text{Al} \rightarrow e^- + \text{Al}$). A conversion signal would require physics beyond the Standard Model. Aim of the experiment is to reach a single event sensitivity of $3 \cdot 10^{-17}$ on the conversion rate. The conversion process results in a monochromatic electron with an energy of 104.973 MeV.

The experiment will use an intense negative muon beam produced starting from a primary 8 GeV kinetic energy proton beam provided by the Fermilab Booster. Protons hit a tungsten target with a power of ~ 8 kW.

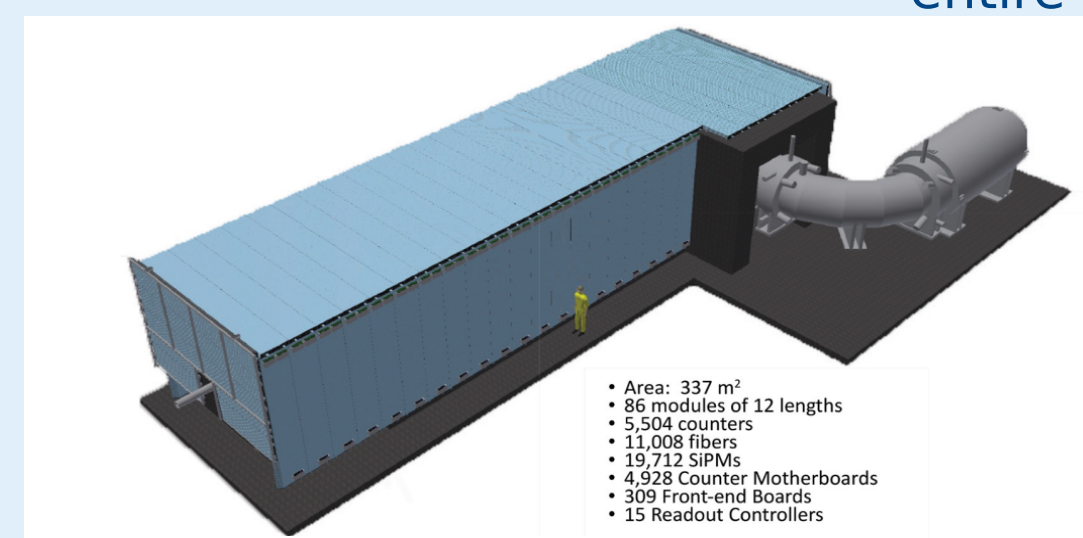
To reduce beam-related backgrounds, a pulsed structure is used (200 ns wide pulses spaced at 1695 ns intervals)

The Cosmic Ray Veto (CRV)

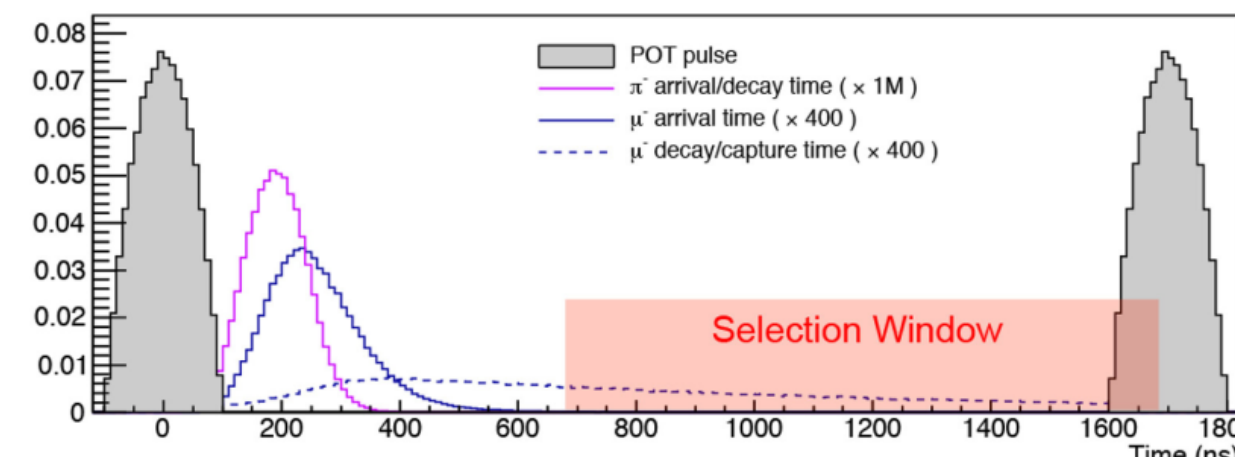
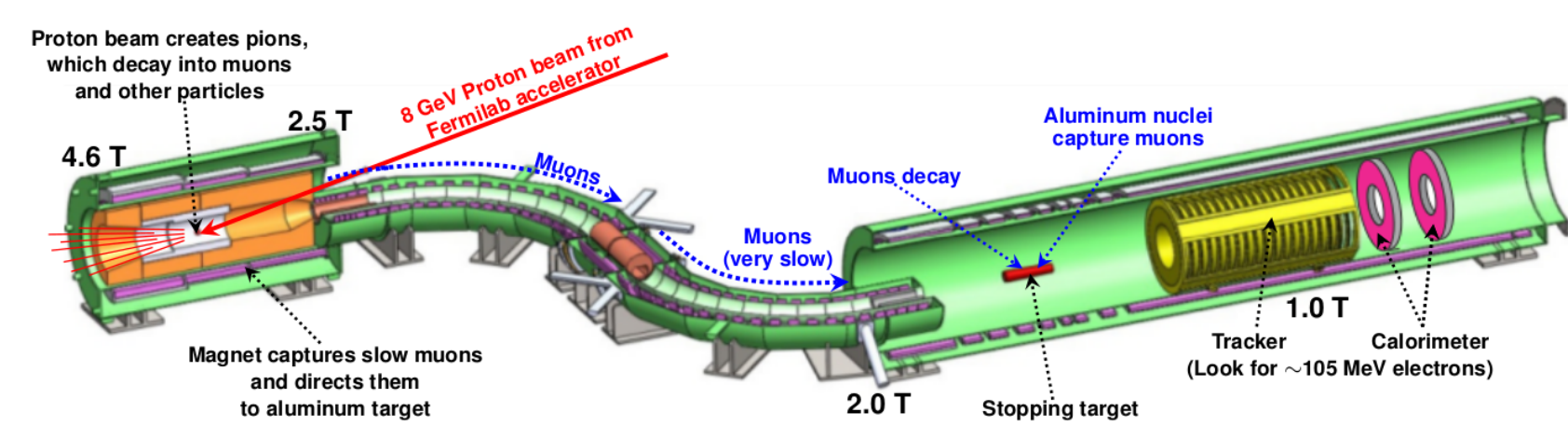
A nearly hermetic cosmic ray veto suppresses the background due to the cosmic rays that could hit the Mu2e stopping target and knock out an electron with the conversion energy (this effect would result in ~ 1 background event per day).

In addition, an electron from a cosmic muon with the conversion energy could be trapped in the field of the TS, propagate in the stopping target region and be reconstructed

The CRV covers therefore entire Detector Solenoid and half of the Transport Solenoid



4 overlapping layers of scintillator bars, with 2 wavelength-shifting fibers/bar



The muon beam is formed through a solenoid system (Production Solenoid, Transport Solenoid and Detector Solenoid). In the picture also the Al Stopping Target, the Tracker and the Calorimeter are shown

The Mu2e beam timing: the proton on target (POT) pulse, with the arrival time of the pions and muons at the Detector Solenoid. The selection window is the time window for the data analysis

In order to reach the desired sensitivity, the **control of the backgrounds** is a critical issue

➔ **Need of very reliable Monte Carlo predictions**

Extensive code-code comparisons between Geant4, FLUKA 2021, MCNP6, MARS15 and PHITS

Beam-related background and key yields

Antiproton background

Proton interactions in the tungsten production target produce antiprotons that could reach the aluminum Stopping target, annihilate and produce background electrons.

In addition, pions created in TS by antiproton interactions can produce background electrons via Radiative Pion Capture (but at least a part of this background can be rejected by a cut on the signal time window).

To control this background, it is crucial the correct evaluation of the number of antiprotons initially forward produced, and then backscattered towards the TS.

Simple problem: To compare Geant4, MCNP, FLUKA and MARS code a monoenergetic, pencil antiproton beam has been assumed, hitting a cylindrical tungsten target of 0.315 cm radius and 16 cm length

Two momentum values for the \bar{p} beam have been considered: 1.9 GeV/c and 2.1 GeV/c

Hadronic models for the \bar{p} production and interaction (when tunable):

- GEANT4 data are produced with the *ShieldingM* physics list
- MCNP simulation uses the LAQGSM03.03 model (as MARS15)

GEANT4 overestimate the \bar{p} yield at large angles

| \bar{p} beam momentum of 1.9 GeV/c | | | | | | | |
|--------------------------------------|----------------------|----------------------|----------|----------------------|----------|----------------------|----------|
| θ | Geant4 | MCNP6 | Δ | FLUKA | Δ | MARS15 | Δ |
| $0^\circ - 10^\circ$ | 3.11 | 3.23 | 3.7% | 3.38 | 8.5% | 3.19 | 2.4% |
| $10^\circ - 45^\circ$ | $5.38 \cdot 10^{-2}$ | $2.28 \cdot 10^{-2}$ | -57.5% | $2.52 \cdot 10^{-2}$ | -53.2% | $1.47 \cdot 10^{-2}$ | -72.6% |
| $45^\circ - 90^\circ$ | $4.43 \cdot 10^{-3}$ | $7.34 \cdot 10^{-4}$ | -83.4% | $1.47 \cdot 10^{-3}$ | -66.9% | $6.42 \cdot 10^{-4}$ | -85.5% |
| $90^\circ - 135^\circ$ | $7.87 \cdot 10^{-5}$ | $3.13 \cdot 10^{-5}$ | -60.3% | $5.47 \cdot 10^{-5}$ | -30.4% | $3.28 \cdot 10^{-5}$ | -58.3% |
| $135^\circ - 180^\circ$ | $8.26 \cdot 10^{-6}$ | $4.57 \cdot 10^{-6}$ | -44.7% | $1.71 \cdot 10^{-6}$ | -79.3% | $6.02 \cdot 10^{-6}$ | -27.1% |

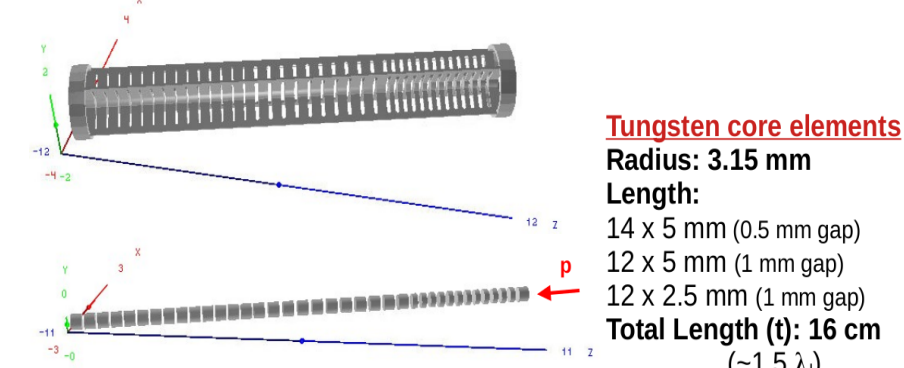
| \bar{p} beam momentum of 2.1 GeV/c | | | | | | | |
|--------------------------------------|----------------------|----------------------|----------|----------------------|----------|----------------------|----------|
| θ | Geant4 | MCNP6 | Δ | FLUKA | Δ | MARS15 | Δ |
| $0^\circ - 10^\circ$ | 3.01 | 3.04 | 1.0% | 3.22 | 7.1% | 3.01 | 0.1% |
| $10^\circ - 45^\circ$ | $5.03 \cdot 10^{-2}$ | $2.27 \cdot 10^{-2}$ | -55.0% | $3.30 \cdot 10^{-2}$ | -34.4% | $1.46 \cdot 10^{-2}$ | -70.9% |
| $45^\circ - 90^\circ$ | $4.12 \cdot 10^{-3}$ | $7.80 \cdot 10^{-4}$ | -81.1% | $1.78 \cdot 10^{-3}$ | -56.8% | $7.09 \cdot 10^{-4}$ | -82.8% |
| $90^\circ - 135^\circ$ | $2.35 \cdot 10^{-4}$ | $3.17 \cdot 10^{-5}$ | -86.5% | $6.70 \cdot 10^{-5}$ | -71.5% | $3.53 \cdot 10^{-5}$ | -84.9% |
| $135^\circ - 180^\circ$ | $3.06 \cdot 10^{-5}$ | $4.20 \cdot 10^{-6}$ | -86.3% | $2.24 \cdot 10^{-6}$ | -92.7% | $6.23 \cdot 10^{-6}$ | -79.7% |

Charged pion yields

One of the most critical parameter to estimate Mu2e sensitivity for conversion electrons (CE) is the number of muons stopped in the Stopping Target:

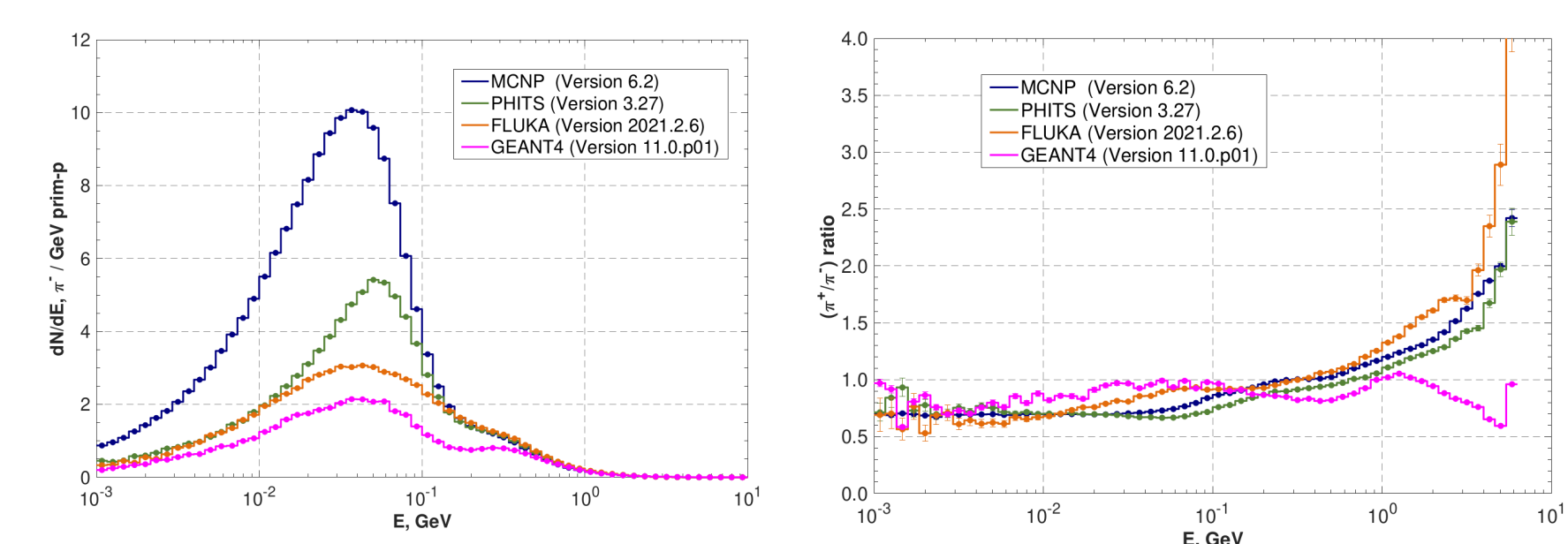
$$N_{\mu^- \text{ POT}} = 1.59 \cdot 10^3$$

This number is highly correlated to the number of π^- produced in the production target and to their angular momentum distribution.



As for the antiproton study, the code-code comparison has been made describing the target as a full cylinder (no gaps, no fins, no magnetic field)

The Mu2e production target

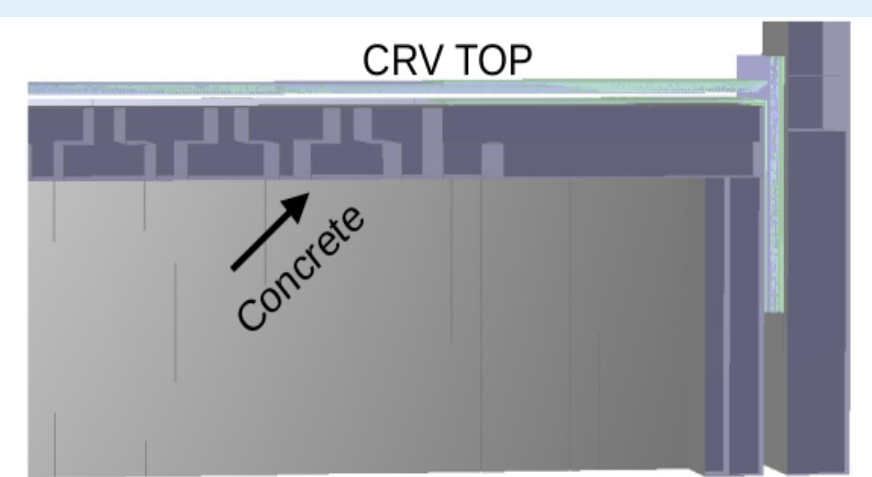


Energy distribution of all π^- exiting the production target (left) and ratio π^+/π^- , evaluated with GEANT4, FLUKA 2021, PHITS and MCNP6

Cosmic rays-related background

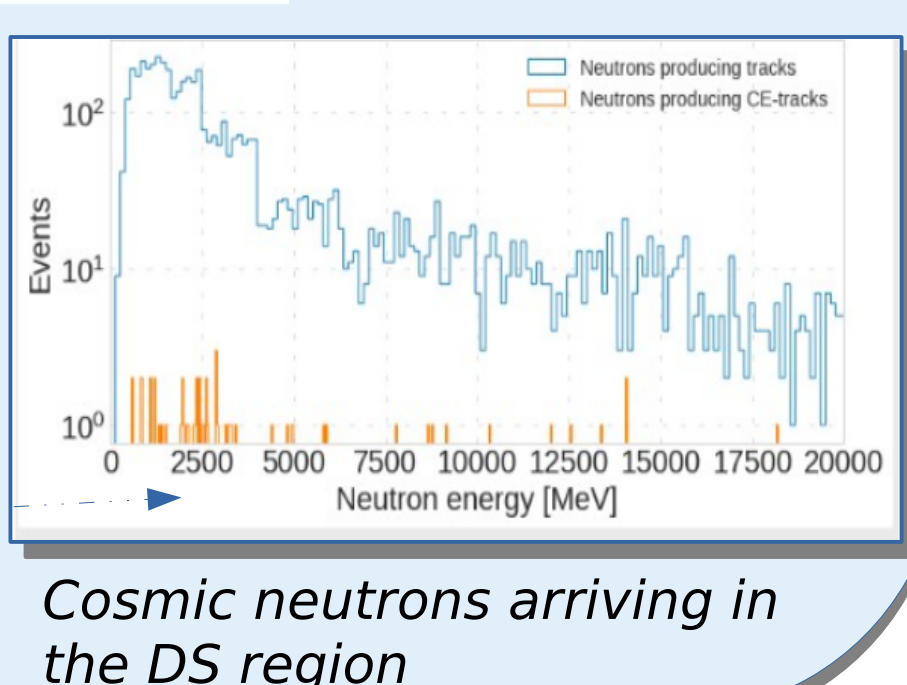
Background induced by the CRV concrete shielding

The CRV system is shielded by 1 m of (normal) concrete, to be protected from the neutrons coming from the upstream beamline



This concrete absorbs cosmic neutrons and neutral kaons, which form an additional possible source of background

Most of the neutrons that via production of secondaries are a possible CE background have an energy of ~ 2.5 GeV

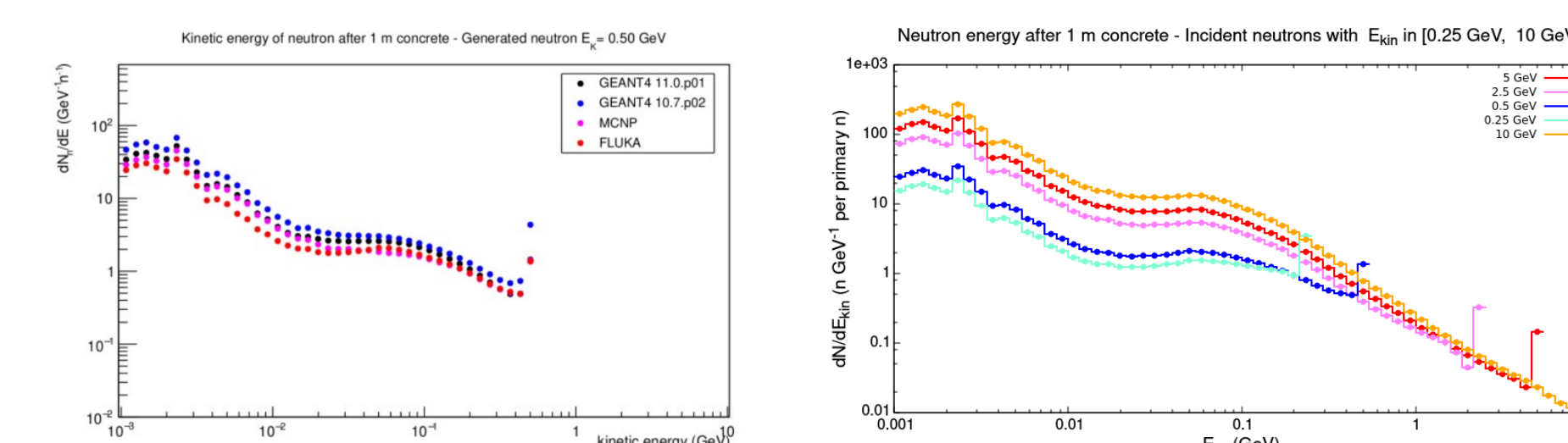


Cosmic neutrons arriving in the DS region

Neutron transmission in concrete

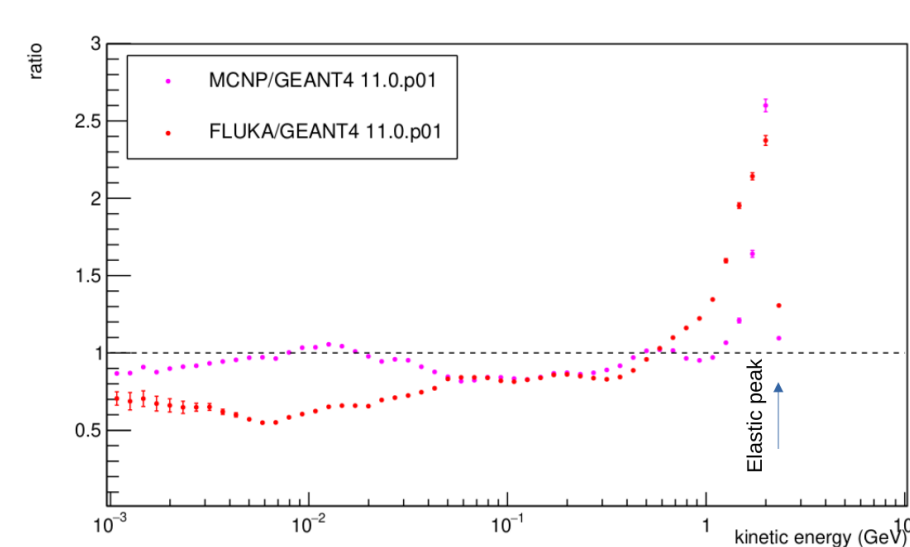
For all transmission simulations, a simple model have been assumed: a slab of concrete 1 m long and with transversal dimensions 10 m x 10 m

Monoenergetic neutron pencil beams have been used as source, with $E_{kin} = 0.25$ GeV, 0.5 GeV, 2.5 GeV, 5.0 GeV and 10 GeV



- The lower value of FLUKA in the low energy range is due to the fact that the coalescence mechanism is taken into account

Spectra of neutrons after 1 m concrete generally differ by less than a factor 2 (but the elastic peak GEANT4 is ~ 2.5 lower than MCNP and FLUKA)

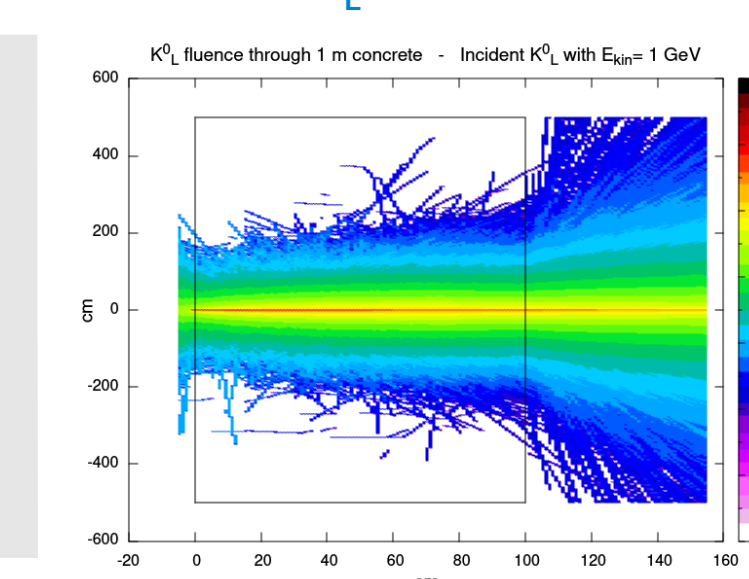


Code-code comparison with $E_{kin}(K^0_L) = 5$ GeV

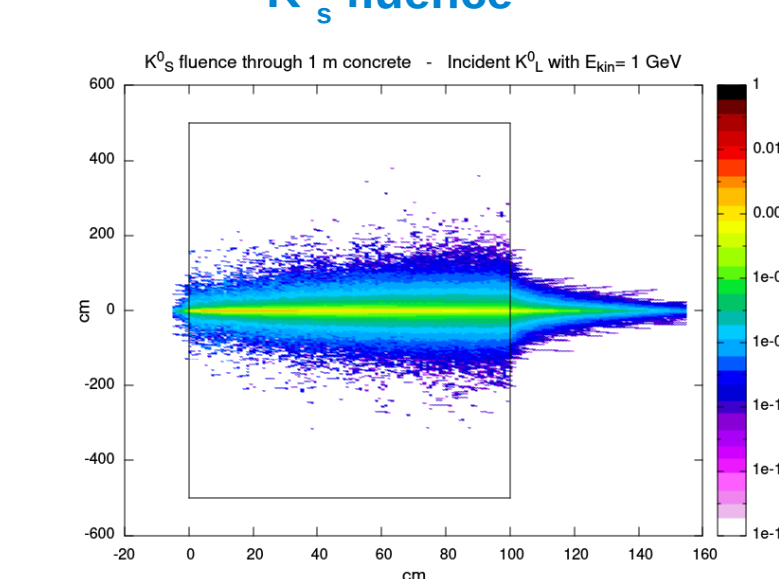
K^0_L transmission in concrete

Monoenergetic neutral kaon pencil beams: $E_{kin} = 10$ MeV, 50 MeV, 100 MeV, 500 MeV and 1 GeV

K^0_L fluence



K^0_S fluence



| | GEANT4 | FLUKA | MCNP |
|---------|--------|-------|------|
| 10 MeV | 0.02% | 7.8% | 30% |
| 50 MeV | 1.7% | 3.4% | 30% |
| 100 MeV | 4.8% | 6.9% | 30% |
| 500 MeV | 4.2% | 9.5% | 19% |
| 1 GeV | 11% | 10% | 18% |

Yield of K^0_L at the elastic peak

At 10 MeV strong discrepancy between GEANT4, FLUKA and MCNP